



A C-type lectin (PvCTL2) from *Penaeus vannamei* participates in antibacterial immune response to *Vibrio parahaemolyticus*

Huan Zhang^{1,2} · Maocang Yan² · Yaohua Wang² · Hui Gao^{1,2} · Lihua Hu² · Dewei Ji² · Min Zhang²

Received: 9 March 2023 / Accepted: 22 June 2023 / Published online: 12 July 2023
© The Author(s), under exclusive licence to Springer Nature Switzerland AG 2023

Abstract

C-type lectin is a type of calcium-dependent sugar recognition protein, which plays an important role in recognizing invading microorganisms as non-self and assists in the clearance of pathogenic microorganisms. In this study, a C-type lectin homolog was identified from *Penaeus vannamei* (*PvCTL2*) using RACE-PCR method and functionally characterized in detail. The open reading frame (ORF) of *PvCTL2* was 1143 bp, encoding 380 amino acids, which contained a conservative carbohydrate recognition domain (CRD) and a low-density lipoprotein receptor (LDLR) domain A. The predicted molecular weight was 41.79 kDa and the theoretical isoelectric point was 6.27. *PvCTL2* was relatively high expressed in muscle, intestine, heart, nerve, and hepatopancreas, and *Vibrio parahaemolyticus* challenge could significantly upregulate the expression level of *PvCTL2* in muscle. Agglutination test of recombinant protein of *PvCTL2* in vitro showed that rPvCTL2 was a Ca²⁺-dependent C-type lectin, which could agglutinate five types of bacteria, including Gram-negative bacteria and fungi, as well as bind different concentrations of monosaccharides. RNAi-based silencing of *PvCTL2* gene resulted in significantly higher mortality rate when shrimp was challenged with *Vibrio parahaemolyticus*, and the median lethal time was significantly shorter than the control. These results suggested that *PvCTL2* could be involved in the immune response against bacterial challenge and contributed to non-self recognition as a pattern recognition receptor in the innate immune system of shrimp *P. vannamei*.

Keywords *Penaeus vannamei* · C-type lectin · Innate immune response · RNA interference

Handling Editor: Pierre Boudry

✉ Min Zhang
milyzhang84@hotmail.com

¹ Zhejiang Ocean University, Zhoushan 316022, China

² Zhejiang Key Laboratory of Exploitation and Preservation of Coastal Bioresource, Wenzhou Key Laboratory of Marine Biological Genetics and Breeding, Zhejiang Mariculture Research Institute, Wenzhou 325005, China

Introduction

Penaeus vannamei is one of the most economically important shrimp species in the world (Alfaro-Montoya et al. 2019). With the continuous changes in the number and scale of shrimp farming, shrimp diseases are continuously emerging, which not only cause direct economic losses to the aquaculture industry but also pollute the ecological environment (Bachère 2000; Muthukrishnan et al. 2019). The common diseases of *P. vannamei* mainly include viral diseases (white spot virus disease, yellow head virus disease, etc.), bacterial diseases (acute hepatopancreas necrosis, larval vibriosis, etc.), and parasitic diseases (*Enterocytozoon hepatopenaei*, EHP) (Walker and Mohan 2009; Abdel-Latif et al. 2022; Flegel 2019; Geetha et al. 2022). These diseases not only increase the mortality rate of shrimp but also limit the sustainable development of the prawn farming industry (Asche et al. 2021). Therefore, in-depth research on disease resistance and immune defense mechanisms in shrimp has become an urgent task for healthy shrimp culture and sustainable development.

In crustacean models (as in other invertebrates), innate immunity mechanisms safeguard the host from “non-self” declared pathogens. The pathogen recognition receptors (PRRs) recognize the pathogen-associated molecular patterns (PAMPs, which are basically carbohydrates on the surface of invading pathogens) and modulate innate immune signals to the cell interior (Dalio et al. 2017; Wang and Wang 2013). Several PRRs have been identified in crustaceans, such as Toll-like receptors (TLRs), peptidoglycan-recognition proteins (PGRPs), Gram-negative binding proteins (GNBPs), lipopolysaccharide and β -1,3-glucan-binding proteins (LGBPs), scavenger receptors (SRs), and lectins. Among the lectin family members, the C-type lectins (CTLs) are the most diverse and best studied (Chai et al. 2018; Kong et al. 2018; Li and Xiang 2013; Pan et al. 2019; Wei et al. 2012). CTLs are a class of calcium-dependent carbohydrate-binding proteins, usually containing one or more carbohydrate recognition domains (CRDs) with 115–130 amino acid residues (Wei et al. 2018; Zhang et al. 2019). CRDs are circular structures connected by two disulfide bonds (Li and Wu 2021) and contain four Ca^{2+} binding sites involved in structure maintenance and carbohydrate binding. Most Ca^{2+} binding sites have conserved “EPN” and “QPD” motifs that can specifically recognize mannose and galactose, respectively. The role of CTLs in innate immunity includes prophenoloxidase induction, cell adhesion, nodule formation, phagocytosis, opsonization enhancement, and cellular encapsulation, as well as microbial clearance and antiviral activity (Guo et al. 2013; Hoving et al. 2014; Yu et al. 2005; Li et al. 2015). In recent years, the involvement of CTLs in the innate immune response of crustaceans has been reported and reviewed (Wang and Wang 2013; Sánchez-Salgado et al. 2017). A CTL from *Portunus trituberculatus* named PtCTL9 can function as an opsonin to promote phagocytosis of blood cells (Kang et al. 2021). PmCL1 from *Penaeus monodon* can promote the clearance of bacteria (Qin et al. 2019), and PmCLec can inhibit the infection of *Vibrio harveyi* (Wongpanya et al. 2017). PcLec2 transcripts from *Procambarus clarkii* participate in the activation of the prophenoloxidase system (Wang et al. 2011). PcLec1, PcLec3, PcLec4, PcLec5, PcLec6, and PcLT participate in antibacterial and antiviral responses (Zhang et al. 2018, 2013, 2011). MjGCTL isolated from *Penaeus japonicus* can bind blood cells to promote cell adhesion and aggregation (Alenton et al. 2017).

Studies on the involvement of CTLs in the innate immune response of *P. vannamei* have also been demonstrated. LvLec1, LvLec2, and LvCLT1 have antiviral activity (Wei et al. 2012; Zhao et al. 2009); LvCTL4.2 and LvCTLU have antibacterial activity,

which can significantly inhibit the growth of *V. parahaemolyticus* (Huang et al. 2022; Song et al. 2019); LvLec can promote phagocytosis, agglutinate blood cells, and also increase the activity of prophenoloxidase (Li et al. 2022); LvLdlrCTL contains a low-density lipoprotein receptor (LDLR) class A domain that has agglutination activity against fungi and bacteria, as well as opsonin activity (Liang et al. 2019). Although some CTLs of *P. vannamei* have been studied, more CTLs need to be characterized. In the present study, the cDNA of a *P. vannamei* CTL (*PvCTL2*) was identified using the rapid amplification of cDNA ends (RACE)-polymerase chain reaction (PCR) approach and the sequence was characterized. The temporal gene expression patterns of *PvCTL2* in response to *V. parahaemolyticus* challenge were tested; the recombinant protein was synthesized using a prokaryotic expression system to analyze bacterial agglutination activity and the inhibition of bacterial agglutination by carbohydrates in vitro. In addition, mortality after silencing of *PvCTL2* through RNA interference under *V. parahaemolyticus* challenge was measured to analyze the role of *PvCTL2* in the shrimp immune system.

Materials and methods

Shrimps

Healthy *P. vannamei* (3.5 ± 0.5 g, 4.7 ± 0.6 cm) were obtained from Yongxing station of Zhejiang Mariculture Research Institute (Zhejiang, China). Before and during the immune challenge, the shrimps were temporarily raised in filtered seawater with 20‰ salinity and continuous aeration at 28.5 ± 0.5 °C. Shrimps were fed with an artificial diet (CP feed, Beihai, Guangxi, China) three times a day (5% of shrimp weight), and 50% seawater was changed every day.

Immune challenge and sample collection

For the immune challenge, shrimps were divided into the control and challenge groups ($n=40$ each). The *V. parahaemolyticus* strain (DX160807) used in this study was isolated and stored by our research group. Each shrimp in the challenge group was injected with 20 μ l of 2×10^7 CFU/ml *V. parahaemolyticus* (48 h LC₅₀) at the abdominal segment, and 20 μ l of 0.9% normal saline was injected into shrimps in the control group. Shrimp muscle tissues were sampled at 0, 3, 6, 12, 24, 48, and 72 h post-infection (hpi), immediately frozen in liquid nitrogen, and stored at -80 °C until further analysis. To eliminate individual differences, at least three shrimps were sampled at each time point. For distribution analysis of *PvCTL2* mRNA in different tissues, shrimps of the control group were dissected into hemocyte, eyestalk, gill, stomach, hepatopancreas, nerve, heart, intestine, and muscle.

Full-length cDNA isolation of PvCTL2

Total RNA was extracted from muscle tissue using *EASYspin* Plus tissue/cell RNA extraction kit (Aidlab, Beijing, China) following the manufacturer's protocol. The quantity and integrity of extracted RNA were measured using a Nano-400

micro-spectrophotometer (Allsheng Instrument, China) and 1.2% agarose gel electrophoresis. The cDNA was synthesized using SMARTer RACE 5'/3' kit (Clontech, USA). The 5' and 3' terminals of *PvCTL2* cDNA were isolated based on 5' RACE and 3' RACE. The full length of *PvCTL2* was amplified using gene-specific primers (PvCTL2F and PvCTL2R, Table 1) and PrimerSTAR and Max DNA Polymerase (TaKaRa, Beijing, China). Then, the purified amplified PCR product was cloned into *pEASY*[®]-Blunt Zero vector (TransGen Biotech, Beijing, China) and sequenced.

cDNA sequence analysis of PvCTL2

The open reading frame (ORF) of *PvCTL2* was predicted by the ORF finder function on the National Center for Biotechnology Information (NCBI) website (<https://www.ncbi.nlm.nih.gov/orffinder/>). The theoretical isoelectric point (pI) and molecular weight (MW) were calculated by ExPASy (<https://web.expasy.org/protparam/>). The Simple Modular Architecture Research Tool (SMART) was used to predict the domains of the deduced PvCTL2 protein. The signal peptide sequence was predicted using SignalP 4.1 (<https://services.healthtech.dtu.dk/service.php?SignalP-4.1>). The ClustalW Multiple Alignment program was used to conduct multiple sequence alignments of PvCTL2 with other CTLs. The percent identity of PvCTL2 with other CTLs was analyzed by the ClustalX version 2.1 program. The phylogenetic tree was constructed by using the neighbor-joining (NJ) method in MEGA 6.0 software based on the CRD sequence of lectins. The number of bootstrap replicates was maintained at 1000.

Table 1 Sequences of the primers used in this study

Primers	Sequence (5'-3')	Utilization
PvCTL2F	TACATGTTATTTTCAGTATCGTGGCGCAATC	cDNA cloning
PvCTL2R	AACGGATAGGCTACACACTGACGATGCTT	cDNA cloning
PvCTL2pCold-F	CCCATATGTTATTTTCAGTATCGTGGCGCA	Protein expression
PvCTL2pCold-R	CCCAAGCTTTCACGGACTGCCAGCGAGCG	Protein expression
PvCTL2-RTF1	TCCAGGACAGACAAGCACCA	qRT-PCR
PvCTL2-RTR1	TGGAGCGTGTCTGTTGAAGGT	qRT-PCR
EF-1 α -F	TATGCTCCTTTTGGACGTTTTGC	Internal reference
EF-1 α -R	CCTTTTCTGCGGCCTTGGTAG	Internal reference
PvCTL2-ds-T7F	GGATCCTAATACGACTCACTATAGGAAGTCTGGTGCTGG CAATGGCA	RNA interference
PvCTL2-ds-R	AGAGGAGGGGAGAGGCACTTGT	RNA interference
PvCTL2-ds-F	AAGTCTGGTGCTGGCAATGGCA	RNA interference
PvCTL2-ds-T7R	GGATCCTAATACGACTCACTATAGGAGAGGGAGAGG CACTTGTT	RNA interference
GFP-ds-T7F	GGATCCTAATACGACTCACTATAGGCGACGTAAACGGCC ACAAGTT	RNA interference
GFP-ds-R	ATGGGGGTGTTCTGCTGGTAG	RNA interference
GFP-ds-F	CGACGTAAACGGCCACAAGTT	RNA interference
GFP-ds-T7R	GGATCCTAATACGACTCACTATAGGATGGGGGTGTTCTG CTGGTAG	RNA interference

Tissue expression and immune challenge analysis of PvCTL2 after *V. parahaemolyticus* challenge

RNAs of tissue samples and muscle samples from the control and the challenge group were isolated, and the cDNAs were prepared using the PrimeScript™ RT reagent kit (with gDNA Eraser). Real-time RT-PCR (RT-qPCR) was performed on a QuantStudio 3 Real-Time PCR System (Applied Biosystems, USA) using the TB Green®Premix Ex Taq™ II kit (TaKaRa, Beijing, China). The specific primers used in the amplification reactions are shown in Table 1. Expression data were normalized to EF-1 α . The expression level of *PvCTL2* was calculated by $2^{-\Delta\Delta CT}$ ($\Delta\Delta CT = \Delta C_{T-PvCTL2} - \Delta C_{T-EF-1\alpha}$) (Livak and Schmittgen 2001).

Expression and purification of recombinant PvCTL2 protein

The ORF of *PvCTL2* was amplified by PCR using specific primers (*pCold I-PvCTL2F* and *pCold I-PvCTL2R*) containing *NdeI* and *HindIII* sites (Table 1). The PrimerSTAR and Max DNA Polymerase were used, and the purified PCR product was ligated into the *pEASY®-Blunt Zero* vector and sequenced. Then, *PvCTL2* was excised from the *pEASY®-Blunt Zero* vector by restriction endonucleases *NdeI* and *HindIII*, respectively, and ligated to *pCold I* by T4 ligase to obtain a recombinant plasmid *pCold I-PvCTL2*.

The recombinant plasmid *pCold I-PvCTL2* was transformed into *Escherichia coli* chaperone-competent cells *pTf16/BL21*. After transformation, bacterial colonies harboring *pCold I-PvCTL2* were selected for rPvCTL2 expression. Cells were cultured in 10 ml Luria–Bertani (LB) medium supplemented with ampicillin (50 $\mu\text{g/ml}$) and chloramphenicol (20 $\mu\text{g/ml}$) overnight at 37 °C. The next day, the bacterial solution was inoculated into 500 ml LB medium supplemented with ampicillin (50 $\mu\text{g/ml}$), chloramphenicol (20 $\mu\text{g/ml}$), and L-arabinose (0.5 mg/ml) until OD₆₀₀ reached 0.6. The culture broth was placed at 15 °C for 30 min and the expression was continued to be induced by adding 0.5 mM IPTG for 24 h. Cells were harvested and resuspended in breaking buffer (20 mM PB, 0.5 M NaCl, 1% Tween 20, 1 mM PMSF) and disrupted by sonication in an ice bath. Then, the proteins were purified by Ni-TED Sefinose™ Resi according to the manufacturer's instructions. The purified proteins were detected using 12% SDS–polyacrylamide gel electrophoresis (SDS-PAGE). The protein concentration was determined by the Bradford assay. To increase the protein concentration, a Amicon® Ultra-4 centrifugal filtration unit (Sigma-Aldrich, Shanghai, China) was used and the purified rPvCTL2 was ultra-filtered according to the manufacturer's instructions. The recombinant protein was stored at –20 °C until use.

Bacterial agglutination and sugar inhibition assays

For testing bacterial agglutination activity, Gram-positive bacteria (*Lactococcus garvieae* strain Y180707), Gram-negative bacteria (*E. coli*, *V. parahaemolyticus* strain DX160807, *V. anguillarum* strain DX210705, *V. tubiashii* strain DX170701), and fungi (*Saccharomyces cerevisiae*) were used; all these strains were stored by our group. Bacteria at the logarithmic phase were collected, stained with 4',6-diamidino-2-phenylindole

(DAPI), then washed three times with TBS and resuspended at the concentration of 2×10^8 CFU/ml. Equal volume of microorganisms-TBS was incubated with purified recombinant rPvCTL2-TBS (final concentration from 20 to 200 $\mu\text{g/ml}$) in the presence of 10 mM CaCl_2 or 10 mM EDTA at 37 °C for 50 min (Kwankaew et al. 2018; Zhang et al. 2009). Agglutination was observed by microscopy. All the assays were performed in triplicate.

To further analyze the inhibitory effect of different sugars on rPvCTL2 agglutinating bacteria, *E. coli* was tested for inhibitory agglutination in the presence of 10 mM CaCl_2 . Equal amounts of rPvCTL2, *E. coli*, and different concentrations of sugars were mixed and incubated at 37 °C for 50 min, and the agglutination was observed under a microscope. The sugars used in the test included D-mannose, D-fructose, D-glucose, D-galactose, sucrose, alginose, and maltose, and the experiments were slightly modified by referring to the method of Liu et al. (2012). All the assays were performed in triplicate.

RNA interference of PvCTL2 and mortality analysis after *V. parahaemolyticus* challenge

Double-stranded RNAs (dsRNAs) specific to *PvCTL2* (dsPvCTL2) and green fluorescent protein (dsGFP, as control) were synthesized by in vitro transcription using a T7 RiboMAX™ Express RNAi System (Promega, USA) based on the primers listed in Table 1. The integrity of dsRNA was confirmed by 1.2% agarose gel electrophoresis, and the concentration and purity were analyzed using a Nano-400 micro-spectrophotometer (Allsheng Instrument, China). RNA interference efficiency of *PvCTL2* or GFP dsRNA was measured by RT-qPCR (EF-1 α as an internal reference). The experimental group was injected with dsPvCTL2 (2 $\mu\text{g/g}$ shrimp), while the control group was injected with dsGFP. Shrimps were collected at 0 hpi, 24 hpi, and 48 hpi, and five shrimps were collected at each time point. The muscle of each shrimp was sampled, and the expression level of *PvCTL2* was measured.

To test the effect of *PvCTL2* in the immune process of *P. vannamei*, the shrimps were divided into the experimental group (dsPvCTL2 + V.P.), control group (dsGFP + V.P.), negative control group (PBS + V.P.), and blank control group (PBS + PBS), with 30 shrimps in each group. The experimental group was injected with 20 μl dsPvCTL2 (2 $\mu\text{g/g}$ shrimp), the control group was injected with 20 μl dsGFP, and the negative control group and blank control group were injected with 20 μl PBS. After 24 h, the experimental group, the control group, and the negative control group were injected with 20 μl of *V. parahaemolyticus* at a concentration of 5×10^6 CFU/ml, and the blank control group was injected with 20 μl of PBS again. Mortality of shrimp was recorded at different time points within 48 h after the second injection.

Statistical analysis

Data on gene expression level and cumulative mortality were processed using the SPSS package (version #16.0) and one-way analysis of variance (ANOVA), followed by the least significant difference (LSD) on the datasets, with the mean value and standard error of the mean (S.E.). The RT-qPCR data and cumulative mortality were plotted using Sigma Plot (version #10).

Results

Characterization of the full-length cDNA of PvCTL2

The full-length cDNA of *PvCTL2* (Accession No. OQ470535) was 1560 bp with an ORF of 1143 bp encoding 380 amino acids. The predicted relative molecular mass of the protein was 41.78 kDa, and the theoretical isoelectric point was 6.27. Analysis result of the SMART program predicted a low-density lipoprotein receptor domain class A (LDLR, 38 aa) at the N-terminal and a CRD of 158 aa at the C-terminal of *PvCTL2* (Fig. 1A, C). Multiple alignments of CRDs in *PvCTL2* with other CTLs showed that *PvCTL2* contained a “QAP” motif that can specifically bind carbohydrates, and four conserved cysteine residues (Cys230, Cys340, Cys356, and Cys364), which could form two disulfide-bonds to stabilize the CRD structure (Fig. 1B).

Percentage identify matrix from multiple alignment analysis of ClustalX version 2.1 showed that *PvCTL2* showed 85% and 84% homology with *PmLdlr* of *P. merguensis* (AUB13319.1) and *PjCTL2* of *P. japonicus* (AFJ59946.1), respectively. Phylogenetic tree analysis of CRDs showed that *PmLdlr* and *PjCTL2* were closely clustered together, formed a sister group to *PvCTL2*, and relatively close to the CTLs from other crustacean species; CTLs of *Azumapecten farreri*, *Macrobrachium rosenbergii*, *Xenopus laevis*, *Homo sapiens*, and *Mus musculus* formed a separate branch in the phylogenetic analysis, and CTLs of *Penaeus merguensis* and *Eriocheir sinensis* formed a completely separate branch in the phylogenetic tree (Fig. 2).

Expression level analysis of PvCTL2 in different tissues and after inoculation with *Vibrio parahaemolyticus*

As shown in Fig. 3A, *PvCTL2* mRNA was ubiquitously expressed in all examined tissues. While the highest expression was noticed in muscle, strikingly lower expression was observed in hemocytes and eyestalk. Furthermore, the response of *PvCTL2* expression in the muscle of pathogen-infected shrimp at different time intervals was also determined (Fig. 3B), the results showed that the mRNA level of *PvCTL2* was significantly upregulated from 3 to 24 hpi, then subsequently decreased to the normal level from 48 to 72 hpi, and the highest expression levels were observed at 6 hpi and 12 hpi which were more than tenfold higher than that at 0 hpi.

Purification of rPvCTL2, bacterial agglutination, and sugar-binding specificity of rPvCTL2

As shown in Fig. 4A, a distinct band of approximately 45 kDa was detected by SDS-PAGE, which indicated that rPvCTL2 was successfully expressed in vitro (Fig. 4A, lane 2, lane 3). Then, rPvCTL2 was successfully purified through a Ni-TED Sefinose™ Resi (Fig. 4B, lane 4). Thereafter, higher purity and concentration of recombinant protein was obtained by an Amicon® Ultra-4 centrifugal filtration (Fig. 4B, lane 5). In the bacterial agglutination analysis, rPvCTL2 (in the presence of 10 mM CaCl₂) agglutinated Gram-negative bacteria (*E. coli*, *V. parahaemolyticus*, *V. anguillarum*, *V. tubiashii*) and fungi (*S. cerevisiae*) (Fig. 5). Agglutination was not observed for all microorganisms tested, in the presence of 10 mM EDTA, suggesting calcium-dependent

(A)

AAGTTATCTCAGTAC

```

1  ATG|TATTTTCAGTATCGTGGCCGACCTCCGCCGAGGATGGACGAACGGCAAGGCGTCTGCTCTTAGGATAAAGAGGCTCAAGCTCATGACACTGTACAGGACCGCGGGACG
1  M L F Q Y R G A I P A S G C D E R Q G A A A L R H K E A V K L M T L S Q E P G T
121 TCAGCTCTTCACGGCTCTGCTTGGGAAGTTTGGAAAGTCACTCCGCTCGTGGCTGCTCTTTGACATAAGACGACCTGCAGATCGAGCCGACGAATGGGGCGCGTGGGAAT
41 S A L S M R F C L G S L E D H S R S C L L F C T K T Q P A D R A A G M G R R G S
241 CTGGTCTGGCAATGGCACTCTTGGACAGTGGCGAAGCCCTGGACTTGGATACATGAGTGGCTCTGGGGACAGATGTGTCAACTTGCATCTCTGTGACGGTGGCAACGAC
81 L V L A M A L L W T A E F A A C D S G Y I R C A S G D R C Y K L A Y I C D G D A C D
361 TGGCGTGCATGTCTGACGAAAACTCTGTTGGTAACAGGACAAACAGACAGCTGAAGCATCTCGAGAACATTCAGGACAGACAGCACCAGGGATGATGACAAACAGCTACGAG
121 G G D M S D E N I C S V T R T N R Q L K H L E T I P G Q T S T T G M M T T T Y E
481 ACCACACTTCTCCGACACCACTCTCCCTCTCCGCCCAACACCTGGAGGAGCGAGGCGTGGTTCAGAGTTCGCTGGACCTTCAACGACACCGCTCCACACCCGAGA
161 T T L P P T T T L P P P P P P N N V E E S E A L G Q R F A R T F N D L H L H P R
601 TGCCCAAGCTCTACACAGCTGGGAAAGTCTCCCTCTCTACTTGTCAAGTCCGCTGGGGGAGCAAGCCCTGTCTGGCCACTCGGCCGAAAGCTGTTGCATAT
201 C P K L Y T S V G N K L S L L Y F V R V G W G E A S A L S A I G G K L V A Y
721 CCTTGGCCCTCGAGGAGAGTTCGCTGCCCTCTCAAGTACTCGGGAGATACAGATGACAGCGACTTCTGGTGGGAGCCGTCACAGAGGACACCGAGGCTGGACGCTGGCTG
241 P S A S E G E F A A L L K Y L R E I Q M T T D F W Y V G G R Y T K D T E A W T W L
841 GACGACCCCGTGCATCGCTCGCCCTACTGGCCGTGACACACCAACAGCTGCAGACCCGACAGGAGTGGCCCAACCGCAAGCTGAAGACTCGCTACTGAGCC
281 D D A P M D L G S P Y W A V R H T N C S S R R Q C E S A P H A R K P E D V A Y W T
961 AACACTTGGCCCTTACCAGTACAGGACGGCGCGCGGCGACTCCAGCAGCTCTGCGCGCCGCTACCTCGCCACTCTTACATATFAGGACAGGAGCTCGCCGGCTCAGG
321 N T S A C Y H Y E Q A P R R D S Q Q L C A A V T F R H Y F Y I S D E D C L G V R
1081 AGCCCTGTGTGACATGTTCCACGACCGCTACGCTACGCTCGCTGGCAGTCTTGA
1361 S P L C E H V P S T A H D L L T A G S P *
GCACCTATGCTTTTCAAAGAAACTTCGGAAGAAATAAAGCCTTGTATATAGTATGATGAATCTTATGAGCAACCTCGTAACTTTTCAATATATGATTTTCAGTAG
CTGTGTTCCAGTAAATACCACTATTTTAAACCAATATGCAATTGCTTGTATAGAAGGGTATGTCAAAATGAAGTCACTTGTAGTACATGAAACAAAGAGGTTTATCTTCT
ATTTCTTTAAAGTACATTTGATGTCATGTAAGTAAACATTTCTACAGATATTTTATAAGATGAATGCCCTTAATAAGCATGTCAGTGTGTACACTCGCTTCTAC
TTTTCTTCCATCTCTCGGCCATCAACGAAGAC

```

(B)

```

PvCTL2 M L F Q Y R G A I P A S G C D E R Q G A A A L R H K E A V K L M T L S Q E P G T S A L S M R F C L G S L E D H S R S C L L F C T K T Q P A D R A A G M G R R G S 100
AEH05998.1 [Panaeus_vannamei] ..... M K R F V L L L C L G F A S A D L G T G E I 23
AUB13319.1 [Panaeus_merguensis] ..... M H R F V S V A L A L L W T A R A C E S G V I 26
ABI97373.1 [Panaeus_monodon] ..... M L L Y L L L F E C S F V S E A D G R V T W N R T L L S Q C C F G G Y I L V G T K C I N F E F A S E T H E A R N F 64
KAG7167775.1 [Homarus_americanus] ..... M L L Y L L L V T C S L F V G E A D G R V T W N R T L L S Q C C F G G Y I L V G T K C I N F E F A S E T H E A R N F 64
ACJ06428.1 [Panaeus_chinensis] ..... M L L Y L L L V T C S L F V G E A D G R V T W N R T L L S Q C C F G G Y I L V G T K C I N F E F A S E T H E A R N F 64

PvCTL2 P C A S G R C R K V L A Y I C G N D C G E M S E E . N I C S V I R . . . . . T N O L K H L E T I P G Q T S T T G M M T T T Y E P F T T L P F P P E . . 173
AEH05998.1 [Panaeus_vannamei] . . . . . A C T S G E R C V P Y V I L C H R D C A D G S D E S P D L C L A W R . N I Q C E R G C A C H A N G D Q C I . S I E A Y C H R T G F A C G S L E R P I S I I R K M S L V S S I S L I P S N 214
AUB13319.1 [Panaeus_merguensis] P C A S G R C R K V L A Y I C G N D C A M S E E . H I G S V I R . . . . . S E R L O R H E A T A G C A T F E I T P T . A T T E L E T T I P F P P E . . 98
ABI97373.1 [Panaeus_monodon] C H A N G I L A I T T A T T L V I L I E N S E L S F T F W E S R E T E E G W L E A S E W S E F F W A R F E C P E N A G N E R L S E F S W E E T W N R V C S M K 144
KAG7167775.1 [Homarus_americanus] A C S E A R K R M K V Y C H R D C A G E D E P E L L V Y E S H F G D R E G V N C R A D R W E C M . K V I N Y C Q D I E F P C E R G N E R L S E F S W E E T W N R V C S M K 164
ACJ06428.1 [Panaeus_chinensis] C H D A G E L A S I T T A T T F R L V E I R A N D L F G R T F V E G R D E E T E G W L I S S E A V E L G T F F W A A F D H Q C P E N S G N E R L S E F S W E E T W N R V C S M K 164
d n

PvCTL2 . . . F N N V E E S E A L G Q R F A R T F N D L H . H E F C K L Y T S G N H S L I L Y F V R V G W G E A S A L S A I G G K L V A Y E S A S G E F A A L L K Y L R E I C M T I T E A G 247
AEH05998.1 [Panaeus_vannamei] . . . D R G V A N K S V E L G S E L R I N L N S T L S . H E F C P F Y T R G G C L S V E Y V S S S G E R S E R H I G E L S I Q N V N . H V D L V N H V N R I T . S G A P 214
AUB13319.1 [Panaeus_merguensis] . . . F N N V E E S E A L G Q R F A R T F N D L H . H E F C K L Y T S G N H S L I L Y F V R V G W G E A S A L S A I G G K L V A Y E S A S G E F A A L L K Y L R E I C M T I T E A G 192
ABI97373.1 [Panaeus_monodon] N E I C E A T V G T E A S A S A L V E F G S A V G R V E L V E L V G L I F W T V E V . C V S A G E L A I D I E . V A R S I F E T C H L S W N R V G 262
KAG7167775.1 [Homarus_americanus] . . . F E S E N K S E Y I G C I L V A L I N N I S I . H E F C H M F Y T G C D S I E S V K V S C R A R N V I N D I L T E K V S . H E S T V C H C L Q C H O L L I T E A G 262
ACJ06428.1 [Panaeus_chinensis] N E I C E A T V G T E A S A S A L V E F G S A V G R V E L A P F V E G L I F L W T V E D T N C C A G T S S L L A I D T E . V E R T I L Y L E I Q A C H O L L I T E A G 262
c v g c w a c 1 f w g

PvCTL2 R Y T K D T E A W T W L D E N I C S V T R T N R Q L K H L E T I P G Q T S T T G M M T T T Y E P F T T L P F P P E . . . . . S A I G G K L V A Y E S A S G E F A A L L K Y L R E I C M T I T E A G 367
AEH05998.1 [Panaeus_vannamei] . . . R Y E V E L S L E D G T E M P R G . S L R R Y E S C N E R N V I L T G S E V R . . . E A N N G E C Y H Y C A E T P F G P E A I T Y D K H Y M S E G E A D M S P G V T A 210
AUB13319.1 [Panaeus_merguensis] R Y T K D T E A W T W L D E N I C S V T R T N R Q S C S R Q C E S A P H A R K P E D V A Y W T N T S A C Y H Y C A E T P F G P E A I T Y D K H Y M S E G E A D M S P G V T A 210
ABI97373.1 [Panaeus_monodon] R Y T K D T E A W T W L D E N I C S V T R T N R Q S C S R Q C E S A P H A R K P E D V A Y W T N T S A C Y H Y C A E T P F G P E A I T Y D K H Y M S E G E A D M S P G V T A 210
KAG7167775.1 [Homarus_americanus] R C M E R G C C T W I D E S A V V C E A V R V E C E S R N V T A R N S T R . V A N S C T R . . . P I L D G L S C Y H Y M S E G E A D M S P G V T A 285
ACJ06428.1 [Panaeus_chinensis] S C L S A S E G T W I T T S E F V E N C H L A D N S A P S . . . . . N G G T S E R L A T G . N F X N F E I N T V S V R K P E C Y R 332
g w g p w c q p d c p l c

PvCTL2 P S T A H E L L I A G S 379
AEH05998.1 [Panaeus_vannamei] V . . . . . 311
AUB13319.1 [Panaeus_merguensis] P S T H E L L I S G G 304
ABI97373.1 [Panaeus_monodon] G . . . . . 333
KAG7167775.1 [Homarus_americanus] G . . . . . 285
ACJ06428.1 [Panaeus_chinensis] G . . . . . 333

```

(C)

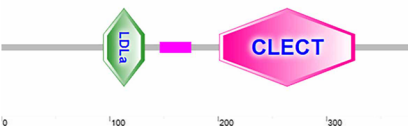


Fig. 1 Sequence analysis of PvCTL2. **A** Nucleotide and deduced amino acid sequences of PvCTL2. The nucleotide (top case) and deduced amino acid (below case) sequences were shown and numbered on the left. Predicted LDLR structures are shaded gray and CRDs are shaded yellow. The start codon and stop codon are surrounded by red boxes. Disulfide bonds are in bold italics. QAP motif is in black box. **B** Alignment of PvCTL2 with C-type lectins from other organisms. *P. vannamei* (AEH05998.1); *P. merguensis* (AUB13319.1); *P. monodon* (ABI97373.1); *Homarus americanus* (KAG7167775.1); *P. chinensis* (ACJ06428.1). **C** The schematic structure of PvCTL2 predicted by SMART program

agglutination process. The minimum concentration required for agglutination was demonstrated against *E. coli* and *V. parahaemolyticus*, followed by *V. tubiashii* and *S. cerevisiae*. The agglutination activity was less against *V. anguillarum*, with no agglutinating activity against *L. garvieae* (Table 2).

Furthermore, the results of sugar-binding specificity showed that agglutinating activity of rPvCTL2 against *E. coli* could be inhibited by the polysaccharide component. The agglutinating activity of rPvCTL2 was found to be inhibited by different concentrations of D-glucose, D-mannose, D-galactose, and D-fructose and not by maltose, trehalose, and maltose (Table 3).

RNA interference of PvCTL2 and its role in innate immunity

To validate the putative role of *PvCTL2* in shrimp innate immunity, RNAi-mediated gene silencing of the transcripts was performed. RT-qPCR results demonstrated that injection of 2 µg/g *dsPvCTL2* suppressed 69% mRNA level of *PvCTL2* in muscle after 48 h (Fig. 6A). After *PvCTL2* was knocked-down, *V. parahaemolyticus* was injected into muscle tissue and the mortality rate was recorded. When compared with the PBS or dsGFP injected groups, cumulative mortality in the *dsPvCTL2* injected group under

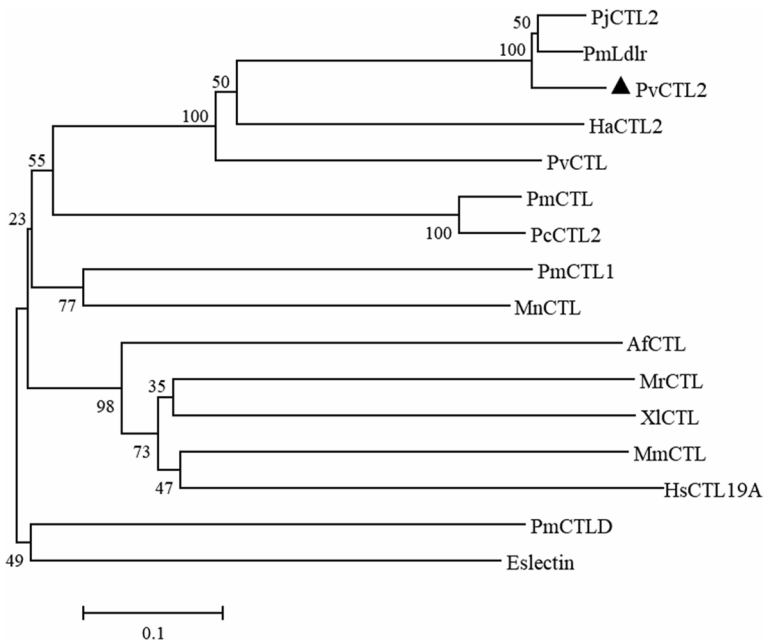


Fig. 2 Phylogenetic tree analysis of CRD region of C-type lectins. PvCTL2 is marked by ▲. The C-type lectin sequences were selected from the following representative species: *Penaeus monodon* (PmCTL, ABI97373.1), *Penaeus chinensis* (PcCTL, ACJ06428.1), *Penaeus merguensis* (PmCTLD, AEB96259.1; PmLdlr, AUB13319.1), *Eriocheir sinensis* (Eslectin, ADB10837.1), *Palaemon modestus* (PmCTL1, AGZ95685.1), *Macrobrachium nipponense* (MnCTL, ARH56436.1), *P. vannamei* (PvCTL, AEH05998.1), *Homarus americanus* (HaCTL2, KAG716775.1), *Penaeus japonicus* (PjCTL2, AFJ59946.1), *Azumapecten farreri* (AfCTL, AAT77680.1), *Macrobrachium rosenbergii* (MrCTL, QJS38721.1), *Xenopus laevis* (XiCTL, BAN13409.1), *Mus musculus* (MmCTL, AAD05125.1), *Homo sapiens* (HsCTL19A, NP_001243649.1)

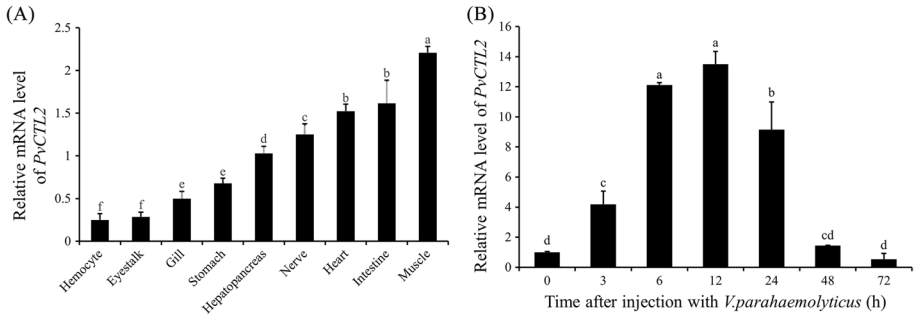


Fig. 3 Expression level analysis of PvCTL2 in different tissues and under immune challenge of *V. parahaemolyticus*. **A** mRNA level of PvCTL2 in hemocyte, eyestalk, gill, stomach, hepatopancreas, nerve, heart, intestine, and muscle. **B** Time-course expression of PvCTL2 in muscle of shrimp challenged by *V. parahaemolyticus* was quantified by real-time RT-PCR. The EF-1 α was used as an internal standard. Bars represented standard errors of mean values. Different letters indicated significant difference ($p < 0.05$, $n = 3$)

V. parahaemolyticus challenge was significantly higher. Mortality rates at 48 hpi were 44%, 67%, and 90%, and the final mortality rates (72 hpi) were 44%, 67%, and 100% for PBS + V.P., *dsGFP* + V.P., and *dsPvCTL2* + V.P., respectively (Fig. 6B).

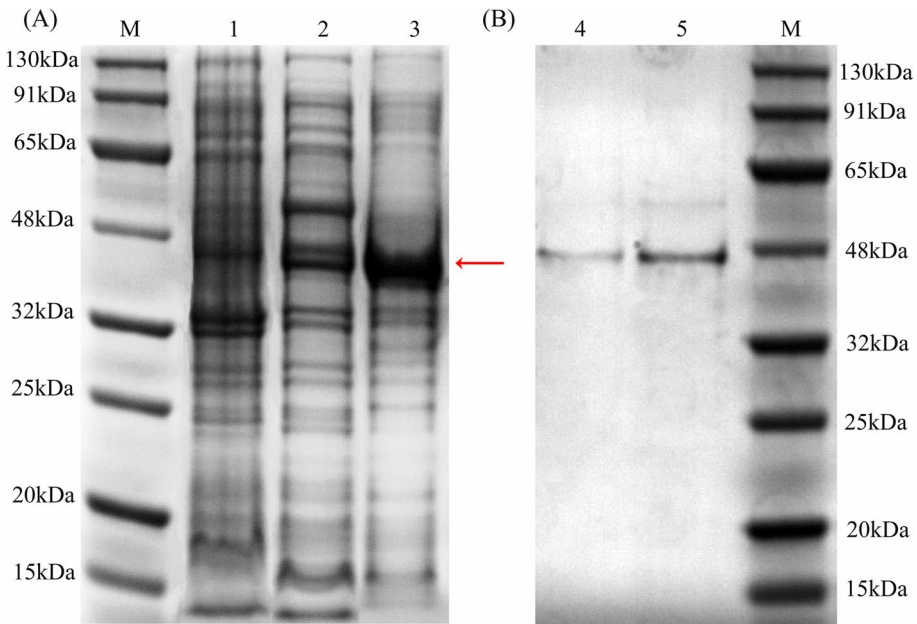


Fig. 4 SDS-PAGE analysis of the rPvCTL2 protein. **(A)** rPvCTL2 induction; **(B)** purification and concentration of rPvCTL2. Lane M: the protein molecular weight marker; lane 1: uninduced *E. coli* transformant expressed pCold I-PvCTL2; lane 2 and lane 3: the supernatant and precipitated proteins, respectively, from *E. coli* with pCold I-PvCTL2; lane 4: the supernatant purified by Ni-TED Sefinose™ Resi; lane 5: rPvCTL2 passed through Amicon® Ultra-4 centrifugal filtration ultrafiltration. The red arrow indicated the location of rPvCTL2

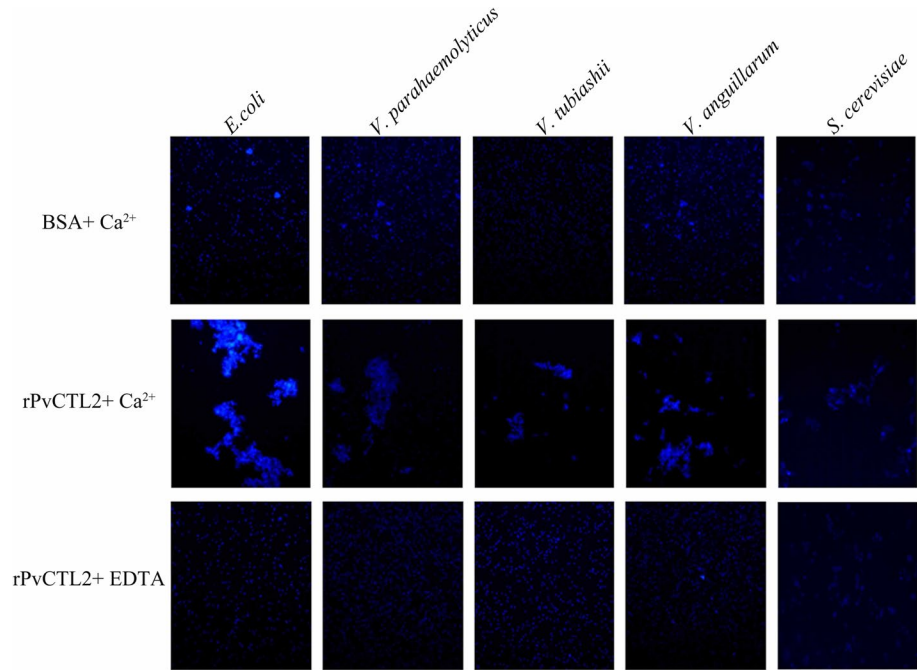


Fig. 5 Agglutination activity of rPvCTL2 on microorganisms. Gram-negative bacteria including *E. coli*, *V. parahaemolyticus* (DX160807), *V. anguillarum* (DX210705), *V. tubiashii* (DX170701), and fungi (*Saccharomyces cerevisiae*) were used for agglutination analysis. The concentration of rPvCTL2 was 200 µg/ml and the BSA (200 µg/ml) was used as a control

Discussion

CTLs are important PRRs, which mediate pathogen recognition and participate in innate immunity. Functional analysis of CTLs in *P. vannamei* has revealed the roles in the immune response to YHV, *V. parahaemolyticus*, and WSSV (Junkunlo et al. 2012; Li et al. 2015,

Table 2 Pathogens agglutinating activity of rPvCTL2

Microorganism	rPvCTL2 (µg/ml)
G+	
<i>Lactococcus garvieae</i>	NA
G–	
<i>Escherichia coli</i>	20
<i>Vibrio parahaemolyticus</i>	20
<i>Vibrio tubiashii</i>	75
<i>Vibrio anguillarum</i>	200
Fungi	
<i>Saccharomyces cerevisiae</i>	75

NA, no agglutination, recombinant protein could not agglutinate bacteria under the maximum detectable concentration (200 µg/ml)

Table 3 Carbohydrate recognition activity of rPvCTL2

Saccharides	rPvCTL2
D-glucose	200 mM
D-mannose	400 mM
D-galactose	50 mM
D-fructose	200 mM
Maltose	NI
Trehalose	NI
Maltose	NI

NI, no inhibition, recombinant protein could not inhibit the bacterial agglutination under the maximum detectable concentration (> 400 mmol/l)

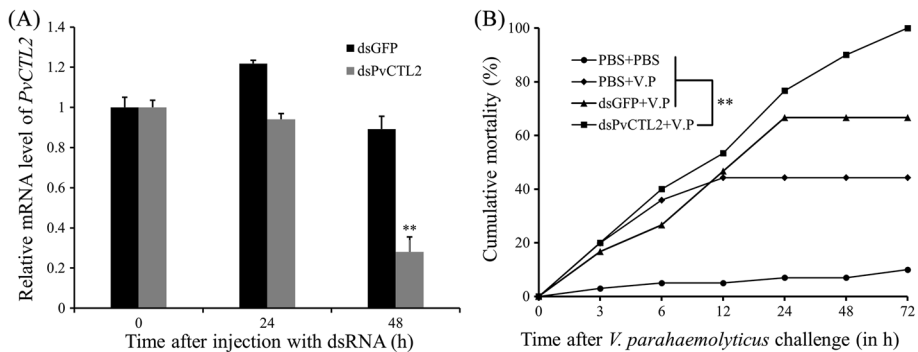


Fig. 6 Silencing analysis of *PvCTL2* in *P. vannamei*. **A** Test the knockdown effect of *PvCTL2* gene by using GFP as control. Examination of *PvCTL2* gene knockdown was conducted using RT-qPCR with EF-1 α as an internal reference. **B** Shrimps of silenced group were injected with ds*PvCTL2* and followed by *V. parahaemolyticus*. Shrimps of control group, negative control group, and blank control group were injected in a similar manner. Bars represent standard errors of mean values. Asterisks indicate significant differences (**: $p < 0.01$, $n = 3$)

2014; Zhao et al. 2009; Song et al. 2019). In current study, we identified and characterized the function of a new CTL named *PvCTL2* in an immune challenge.

PvCTL2 is a protein composed of 380 amino acids; the predicted protein sequence contains an LDLR class A domain and a CRD. This LDLR functions in regulating cholesterol homeostasis through receptor-mediated endocytosis of lipoproteins particles (May et al. 2007). The LDLR class A domains are known to bind low-density lipoprotein and calcium (Fass et al. 1997). The immune effects of CTLs that contain LDLR domain in crustaceans include the activation of phenoloxidase progenitor system, antibacterial, and antiviral responses (Junkunlo et al. 2012; Huang et al. 2014; Xu et al. 2014). Among these CTLs, *LdlrCTL* and *LvCTLD* are from *P. vannamei*, and deletion of LDLR in *LvLdlrCTL* results in lower phagocytosis of hemocytes which indicates its potential role in the immune response. Further investigation of the LDLR domain in the immune response is still required. The CTLD is located at the C-terminal of *PvCTL2* and its structure is mainly maintained by four conserved cysteine residues that form two disulfide bonds (Zelensky and Gready 2005). CTLs are generally thought to possess a CRD of 115–130 amino acids, but the CRD of *PvCTL2* is longer than the normal range, with 158 amino acids. In the

phylogenetic tree, PvCTL2 was clustered together CTLs from *P. japonicus* and *P. merquensis*. The structural features and relationships displayed in the BLAST results and phylogenetic tree suggested that PvCTL2 is a new member of the CTL superfamily of *P. vannamei*.

Aggregation activity is the most important feature of CTLs. In the presence of calcium, rPvCTL2 agglutinated Gram-negative bacteria (*E. coli*, *V. parahaemolyticus*, *V. anguillarum*, *V. tamarii*) and fungi (*S. cerevisiae*). According to previous studies, other CTLs containing LDLR domains also agglutinate bacteria. For example, both MnCTLDcp2 from *Macrobrachium nipponense* (Xiu et al. 2015) and EsCTLDcp from *Eriocheir sinensis* (Huang et al. 2014) can agglutinate Gram-positive (*S. aureus*) and Gram-negative bacteria (*Aeromonas hydrophila* and *V. parahaemolyticus*). Compared with the reported CTLs, rPvCTL2 showed a broader spectrum of pathogenic bacteria agglutinating activity. Most CRDs possess “EPN” and “QPD” binding motifs that are specific for mannose and galactose, respectively. Although PvCTL2 had a “QPD” mutation in the “QAP” motif, sugar inhibition assays revealed that rPvCTL2 could bind to D-fructose, D-galactose, D-glucose, and D-mannose, thereby inhibiting the binding of rPvCTL2 with *E. coli*. These results showed that rPvCTL2 had agglutinating activity and was involved in defense against various bacterial pathogens in a calcium-dependent and carbohydrate-dependent manner.

PvCTL2 was expressed in wide range of tissues suggesting its importance in immune defense of the host. Furthermore, high *PvCTL2* mRNA level was found in muscle, intestine, heart, nerve, and hepatopancreas, which was quite different from other CTLs in *P. vannamei* since most of them were highly expressed in hepatopancreas, gill, or hemocyte. However, relative high expression level of *Lvlectin-1* and *LvCTL7* also have been found in muscle tissue (Wei et al. 2012; Luo et al. 2023). Furthermore, after *V. parahaemolyticus* challenge, the expression level of *PvCTL2* in muscle was significantly upregulated from 3 to 24 hpi. Although the muscle is not the immune organ in the shrimp, the result indicated that *PvCTL2* played an important role in bacteria defense in this tissue. However, the role of *PvCTL2* in immune defense still needs to be studied in detail since we did not determine the mRNA level change in other tissues. Considering the result that rPvCTL2 could bind *V. parahaemolyticus* in vitro, this study suggested that *PvCTL2* could be efficiently induced by *V. parahaemolyticus* to promote recognition or clearance of invading bacteria. Similarly, for most other CTLs from *P. vannamei*, bacterial or viral challenge can also effectively induce the expression of these CTLs. Furthermore, RNAi was used to analyze the function of *PvCTL2* in vivo. The result showed that injection of dsPvCTL2 into the muscle of *P. vannamei* could efficiently reduce the expression of *PvCTL2*, and silence of *PvCTL2* significantly increased the cumulative mortality after *V. parahaemolyticus* challenge. These results suggested the involvement of *PvCTL2* in shrimp immunity against bacterial challenge.

Conclusions

In summary, a new LDLa domain-containing CTL (*PvCTL2*) was cloned from *P. vannamei*. The expression level of *PvCTL2* was regulated by bacterial challenge, and the recombinant protein agglutinated various bacteria in a calcium-dependent manner. All these results suggested that *PvCTL2* could function as a PRR involved in the agglutination and antibacterial immunity of *P. vannamei*.

Author contribution All authors contributed to the study conception and design. Experiment design, data collection, and analysis were performed by Huan Zhang, Yaohua Wang, Maocang Yan, and Min Zhang. Hui Gao performed the gene expression analysis. Material preparation was performed by Lihua Hu and Dewei Ji. The first draft of the manuscript was written by Huan Zhang and Min Zhang, and all authors commented on previous versions of the manuscript. All authors read and approved the final manuscript.

Funding The present study was supported by the Key Scientific and Technological Grant of Zhejiang for Breeding New Agricultural Varieties (No. 2021C02069-5), Wenzhou Breeding Cooperation Group Project of New Agricultural Products (No. 2019ZX002-01), and Wenzhou Science and Technology Project (No. N20210022).

Data availability All data generated or analyzed during this study are included in this published article and its supplementary information files.

Declarations

Competing interests The authors declare no competing interests.

References

- Abdel-Latif HM, Yilmaz E, Dawood MA, Ringø E, Ahmadifar E, Yilmaz S (2022) Shrimp vibriosis and possible control measures using probiotics, postbiotics, prebiotics, and synbiotics: a review. *Aquaculture* 551:737951. <https://doi.org/10.1016/j.aquaculture.2022.737951>
- Alenton RRR, Koiwai K, Miyaguchi K, Kondo H, Hirono I (2017) Pathogen recognition of a novel C-type lectin from *Marsupenaeus japonicus* reveals the divergent sugar-binding specificity of QAP motif. *Sci Rep* 7:1–11. <https://doi.org/10.1038/srep45818>
- Alfaro-Montoya J, Braga A, Umaña-Castro R (2019) Research frontiers in penaeid shrimp reproduction: future trends to improve commercial production. *Aquaculture* 503:70–87. <https://doi.org/10.1016/j.aquaculture.2018.12.068>
- Asche F, Anderson JL, Botta R, Kumar G, Abrahamsen EB, Nguyen LT, Valderrama D (2021) The economics of shrimp disease. *J Invertebr Pathol* 186:107397. <https://doi.org/10.1016/j.jip.2020.107397>
- Bachère E (2000) Shrimp immunity and disease control. *Aquaculture* 191:3–11. [https://doi.org/10.1016/S0044-8486\(00\)00413-0](https://doi.org/10.1016/S0044-8486(00)00413-0)
- Chai LQ, Meng JH, Gao J, Xu YH, Wang XW (2018) Identification of a crustacean β -1,3-glucanase related protein as a pattern recognition protein in antibacterial response. *Fish Shellfish Immunol* 80:155–164. <https://doi.org/10.1016/j.fsi.2018.06.004>
- Dalio RJD, Magalhães DM, Rodrigues CM, Arena GD, Oliveira TS, Souza-Neto RR, Picchi SC, Martins PMM, Santos PJC, Maximo HJ, Pacheco IS, De Souza AA, Machado MA (2017) PAMPs, PRRs, effectors and R-genes associated with citrus–pathogen interactions. *AOB* 119:749–774. <https://doi.org/10.1093/aob/mcw238>
- Flegel TW (2019) A future vision for disease control in shrimp aquaculture. *J World Aquacult Soc* 50:249–266. <https://doi.org/10.1111/jwas.12589>
- Geetha R, Avunje S, Solanki HG, Priyadarshini R, Vinoth S, Anand RP, Ravisankar T, Patil PK (2022) Farm-level economic cost of *Enterocytozoon hepatopenaei* (EHP) to India *Penaeus vannamei* shrimp farming. *548*: 737685. <https://doi.org/10.1016/j.aquaculture.2021.737685>
- Guo XN, Jin XK, Li S, Yu AQ, Wu MH, Tan SJ, Zhu YT, Li WW, Zhang P, Wang Q (2013) A novel C-type lectin from *Eriocheir sinensis* functions as a pattern recognition receptor with antibacterial activity. *Fish Shellfish Immunol* 35:1554–1565. <https://doi.org/10.1016/j.fsi.2013.08.021>
- Hoving JC, Wilson GJ, Brown GD (2014) Signalling C-type lectin receptors, microbial recognition and immunity. *Cell Microbiol* 16:185–194. <https://doi.org/10.1111/cmi.12249>
- Huang Y, An L, Hui K-M, Ren Q, Wang W (2014) An LDLa domain-containing C-type lectin is involved in the innate immunity of *Eriocheir sinensis*. *Dev Comp Immunol* 42:333–344. <https://doi.org/10.1016/j.dci.2013.10.004>
- Huang YH, Kumar R, Liu CH, Lin SS, Wang HC (2022) A novel C-type lectin LvCTL 4.2 has antibacterial activity but facilitates WSSV infection in shrimp (*L. vannamei*). *Dev Comp Immunol* 126:104239. <https://doi.org/10.1016/j.dci.2021.104239>

- Junkunlo K, Prachumwat A, Tangprasittipap A, Senapin S, Borwornpinyo S, Flegel TW, Sritunyaluck-sana K (2012) A novel lectin domain-containing protein (LvCTLTD) associated with response of the whiteleg shrimp *Penaeus (Litopenaeus) vannamei* to yellow head virus (YHV). *Dev Comp Immunol* 37:334–341. <https://doi.org/10.1016/j.dci.2011.12.010>
- Kang T, Xia Y, Dong T, Zheng X, Yang S, Qian S, Huang M, Fei H (2021) C-type lectin with a QPN motif from swimming crab *Portunus trituberculatus* displays broad nonself-recognition ability and functions as an opsonin. *Dev Comp Immunol* 120:104066. <https://doi.org/10.1016/j.dci.2021.104066>
- Kong T, Gong Y, Liu Y, Wen X, Tran NT, Aweya JJ, Zhang Y, Ma H, Zheng H, Li S (2018) Scavenger receptor B promotes bacteria clearance by enhancing phagocytosis and attenuates white spot-syndrome virus proliferation in *Scylla paramamosian*. *Fish Shellfish Immunol* 78:79–90. <https://doi.org/10.1016/j.fsi.2018.04.027>
- Kwankaew P, Praparatana R, Runsaeng P, Utarabhand P (2018) An alternative function of C-type lectin comprising low-density lipoprotein receptor domain from *Fenneropenaeus merguensis* to act as a binding receptor for viral protein and vitellogenin. *Fish Shellfish Immunol* 74:295–308. <https://doi.org/10.1016/j.fsi.2017.12.044>
- Li D, Wu M (2021) Pattern recognition receptors in health and diseases. *STTT* 6:291. <https://doi.org/10.1038/s41392-021-00687-0>
- Li F, Xiang J (2013) Recent advances in researches on the innate immunity of shrimp in China. *Dev Comp Immunol* 39:11–26. <https://doi.org/10.1016/j.dci.2012.03.016>
- Li M, Li CZ, Ma CX, Li HY, Zuo HL, Weng SP, Chen XH, Zeng DG, He JG, Xu XP (2014) Identification of a C-type lectin with antiviral and antibacterial activity from Pacific white shrimp *Litopenaeus vannamei*. *Dev Comp Immunol* 46:231–240. <https://doi.org/10.1016/j.dci.2014.04.014>
- Li H, Chen Y, Li M, Wang S, Zuo H, Xu X, Weng S, He J, Li C (2015) A C-type lectin (LvCTLA) from *Litopenaeus vannamei* is a downstream molecule of the NF- κ B signaling pathway and participates in antibacterial immune response. *Fish Shellfish Immunol* 43:257–263. <https://doi.org/10.1016/j.fsi.2014.12.024>
- Li Y, Pan L, Yu J (2022) The injection of one recombinant C-type lectin (LvLec) induced the immune response of hemocytes in *Litopenaeus vannamei*. *Fish Shellfish Immunol* 124:324–331. <https://doi.org/10.1016/j.fsi.2022.04.017>
- Liang Z, Yang L, Zheng J, Zuo H, Weng S, He J, Xu X (2019) A low-density lipoprotein receptor (LDLR) class A domain-containing C-type lectin from *Litopenaeus vannamei* plays opposite roles in antibacterial and antiviral responses. *Dev Comp Immunol* 92:29–34. <https://doi.org/10.1016/j.dci.2018.11.002>
- Liu YC, Liu LJ, Zhang YC, Geng XY, Sun Y, Sun JS (2012) Recombinant expression and functional characterization of a C-type lectin (*Fclectin*) from the Chinese shrimp (*Fenneropenaeus chinensis*). *J Fisheries China* 36:1493–1502. <https://doi.org/10.3724/SP.J.1231.2012.28102>
- Livak KJ, Schmittgen TD (2001) Analysis of relative gene expression data using real-time quantitative PCR and the 2 $^{-\Delta\Delta CT}$ method. *Methods* 25:402–408. <https://doi.org/10.1006/meth.2001.1262>
- Luo JL, Chen YH, Huang YX, Feng JM, Yuan YH, Jjian JC, Cai SH, Yang SP (2023) A novel C-type lectin for *Litopenaeus vannamei* in the innate immune response against *Vibrio* infection. *Fish Shellfish Immunol* 135:108621. <https://doi.org/10.1016/j.fsi.2023.108621>
- May P, Woldt E, Matz RL, Boucher P (2007) The LDL receptor-related protein (LRP) family: an old family of proteins with new physiological functions. *Ann Med* 39:219–228. <https://doi.org/10.1080/07853890701214881>
- Muthukrishnan S, Defoirdt T, InaSalwany MY, Yusoff FM, Shariff M, Ismail SI, Natrah I (2019) *Vibrio parahaemolyticus* and *Vibrio harveyi* causing acute hepatopancreatic necrosis disease (AHPND) in *Penaeus vannamei* (Boone, 1931) isolated from Malaysian shrimp ponds. *Aquaculture* 511:734227. <https://doi.org/10.1016/j.aquaculture.2019.734227>
- Pan XT, Li TT, Yang CH, Ren Q, Zhang XW (2019) A toll receptor is involved in antibacterial defense in the oriental river prawn, *Macrobrachium nipponense*. *Fish Shellfish Immunol* 92:583–589. <https://doi.org/10.1016/j.fsi.2019.06.042>
- Qin Y, Jiang S, Huang J, Zhou F, Yang Q, Jiang S, Yang L (2019) C-type lectin response to bacterial infection and ammonia nitrogen stress in tiger shrimp (*Penaeus monodon*). *Fish Shellfish Immunol* 90:188–198. <https://doi.org/10.1016/j.fsi.2019.04.034>
- Sánchez-Salgado JL, Pereyra MA, Agundis C, Vivanco-Rojas O, Sierra-Castillo C, Alpuche-Osorno JJ, Zenteno E (2017) Participation of lectins in crustacean immune system. *Aquac Res* 48:4001–4011. <https://doi.org/10.1111/are.13394>
- Song F, Chen GL, Lu KC, Fan JQ, Yan MT, He HH, Lian YY, Zhang CZ, Chen YH (2019) Identification and functional characterization of a C-type lectin gene from *Litopenaeus vannamei* that is

- associated with ER-stress response. *Fish Shellfish Immunol* 93:977–985. <https://doi.org/10.1016/j.fsi.2019.08.056>
- Walker PJ, Mohan CV (2009) Viral disease emergence in shrimp aquaculture: origins, impact and the effectiveness of health management strategies. *Rev Aquacul* 1:125–154. <https://doi.org/10.1111/j.1753-5131.2009.01007.x>
- Wang XW, Wang JX (2013) Diversity and multiple functions of lectins in shrimp immunity. *Dev Comp Immunol* 39:27–38. <https://doi.org/10.1016/j.dci.2012.04.009>
- Wang XW, Zhang HW, Li X, Zhao XF, Wang JX (2011) Characterization of a C-type lectin (PcLec2) as an upstream detector in the prophenoloxidase activating system of red swamp crayfish. *Fish Shellfish Immunol* 30:241–247. <https://doi.org/10.1016/j.fsi.2010.10.012>
- Wei X, Liu X, Yang J, Fang J, Qiao H, Zhang Y, Yang J (2012) Two C-type lectins from shrimp *Litopenaeus vannamei* that might be involved in immune response against bacteria and virus. *Fish Shellfish Immunol* 32:132–140. <https://doi.org/10.1016/j.fsi.2011.11.001>
- Wei X, Wang L, Sun W, Zhang M, Ma H, Zhang Y, Zhang X, Li S (2018) C-type lectin B (*SpCTL-B*) regulates the expression of antimicrobial peptides and promotes phagocytosis in mud crab *Scylla paramamosain*. *Dev Comp Immunol* 84:213–229. <https://doi.org/10.1016/j.dci.2018.02.016>
- Wongpanya R, Sengprasert P, Amparyup P, Tassanakajon A (2017) A novel C-type lectin in the black tiger shrimp *Penaeus monodon* functions as a pattern recognition receptor by binding and causing bacterial agglutination. *Fish Shellfish Immunol* 60:103–113. <https://doi.org/10.1016/j.fsi.2016.11.042>
- Xiu Y, Hou L, Liu X, Wang Y, Gu W, Meng Q, Wang W (2015) Isolation and characterization of two novel C-type lectins from the oriental river prawn, *Macrobrachium nipponense*. *Fish Shellfish Immunol* 46:603–611. <https://doi.org/10.1016/j.fsi.2015.07.011>
- Xu YH, Bi WJ, Wang XW, Zhao YR, Zhao XF, Wang JX (2014) Two novel C-type lectins with a low-density lipoprotein receptor class A domain have antiviral function in the shrimp *Marsupenaeus japonicus*. *Dev Comp Immunol* 42:323–332. <https://doi.org/10.1016/j.dci.2013.10.003>
- Yu X-Q, Tracy ME, Ling E, Scholz FR, Trenczek T (2005) A novel C-type immunlectin-3 from *Manduca sexta* is translocated from hemolymph into the cytoplasm of hemocytes. *Insect Biochem Molec* 35:285–295. <https://doi.org/10.1016/j.ibmb.2005.01.004>
- Zelensky AN, Gready JE (2005) The C-type lectin-like domain superfamily. *FEBS Lett* 272:6179–6217. <https://doi.org/10.1111/j.1742-4658.2005.05031.x>
- Zhang XW, Xu WT, Wang XW, Mu Y, Zhao XF, Yu XQ, Wang JX (2009) A novel C-type lectin with two CRD domains from Chinese shrimp *Fenneropenaeus chinensis* functions as a pattern recognition protein. *Mol Immunol* 46:1626–1637. <https://doi.org/10.1016/j.molimm.2009.02.029>
- Zhang XW, Wang XW, Sun C, Zhao XF, Wang JX (2011) C-type lectin from red swamp crayfish *Procambarus clarkii* participates in cellular immune response. *Arch Insect Biochem* 76:168–184. <https://doi.org/10.1002/arch.20416>
- Zhang XW, Ren Q, Zhang HW, Wang KK, Wang JX (2013) A C-type lectin could selectively facilitate bacteria clearance in red swamp crayfish, *Procambarus clarkii*. *Fish Shellfish Immunol* 35:1387–1394. <https://doi.org/10.1016/j.fsi.2013.08.004>
- Zhang XW, Man X, Huang X, Wang Y, Song QS, Hui KM, Zhang HW (2018) Identification of a C-type lectin possessing both antibacterial and antiviral activities from red swamp crayfish. *Fish Shellfish Immunol* 77:22–30. <https://doi.org/10.1016/j.fsi.2018.03.015>
- Zhang X, Pan L, Yu J, Huang H (2019) One recombinant C-type lectin (*LvLec*) from white shrimp *Litopenaeus vannamei* affected the haemocyte immune response *in vitro*. *Fish Shellfish Immunol* 89:35–42. <https://doi.org/10.1016/j.fsi.2019.03.029>
- Zhao ZY, Yin ZX, Xu XP, Weng SP, Rao XY, Dai ZX, Luo YW, Yang G, Li ZS, Guan HJ, Li SD, Ch-an SM, Yu XQ, He JG (2009) A novel C-type lectin from the shrimp *Litopenaeus vannamei* possesses anti-white spot syndrome virus activity. *J Virol* 83:347–356. <https://doi.org/10.1128/JVI.00707-08>

Publisher's note Springer Nature remains neutral with regard to jurisdictional claims in published maps and institutional affiliations.

Springer Nature or its licensor (e.g. a society or other partner) holds exclusive rights to this article under a publishing agreement with the author(s) or other rightsholder(s); author self-archiving of the accepted manuscript version of this article is solely governed by the terms of such publishing agreement and applicable law.